Optimizing photocatalytic degradation of phenol by TiO₂/GAC using response surface methodology

Jin-Chung Sin, Sze-Mun Lam, and Abdul Rahman Mohamed[†]

School of Chemical Engineering, Universiti Sains Malaysia, Engineering Campus,
14300 Nibong Tebal, Pulau Pinang, Malaysia

Abstract−TiO₂ deposited on granular activated carbon (TiO₂/GAC) was used for photocatalytic degradation of phenol. The effects of photocatalyst loading, initial substrate concentration and addition of an oxidizing agent as H_2O_2 were investigated using a one-factor-at-a-time experiment. Central composite design, an experimental design for response surface methodology (RSM), was used for the modelling and optimization of the phenol degradation. Analysis of variance (ANOVA) indicated that the proposed quadratic model was in agreement with the experimental case with R^2 and R^2_{adj} correlation coefficients of 0.9760 and 0.9544, respectively. Accordingly, the optimum conditions for phenol degradation were a photocatalyst loading of two layers, initial phenol concentration of 34.44 mg L^{-1} and H_2O_2 concentration of 326.90 mg L^{-1}. The TiO₂/GAC was used for five cycles with phenol degradation efficiency still higher than 90%. Finally, the phenol that remained adsorbed on GAC was able to migrate to TiO₂ and then photocatalytically be degraded.

Key words: TiO₂, Granular Activated Carbon, Phenol, Photocatalytic Degradation, Response Surface Methodology

INTRODUCTION

Contamination of water by phenol and its derivatives is a serious problem experienced by nations throughout the developed and developing countries. Phenols have been widely used by many industries such as petrochemical, petroleum refineries, phenolic resin manufacturing, textile, paint, plastic, paper-making and iron smelting [1]. The releases of these untreated organic pollutants into the environment are of high priority concern since they are harmful to organisms at low concentrations and many of them have been listed as hazardous pollutants by both the US Environmental Protection Agency and the European Commission [2,3]. The ingestion of such contaminated water into the human body also can cause paralysis of the central nervous system and damage the kidney, liver and pancreas [4]. Due to their high toxicity and recalcitrant nature, the removal to innocuous levels is an arduous process for many biological, physical and chemical processes [5,6]. Therefore, suitable and efficient wastewater treatment methods for removing the phenols from the wastewater must be considered.

The use of the heterogeneous photocatalysis for the oxidation of organic and inorganic pollutants in both water and air has been actively studied in the past 20 years [2,5,7-12]. The preferential use of TiO₂ for the photocatalytic degradation of organic pollutants is based on its low cost, non-toxicity and photochemical stability. This process is based on the formation of nonselective and highly reactive radicals such as hydroxyl radicals (•OH), which can attack a wide range of organic pollutants by converting them into carbon dioxide, water and other associated inorganic salts. However, fine TiO₂ powder is generally accompanied by complications arising from the need for separation of the powder from the treated pollutants, which prevents the large-scale applications of this promising method.

Several efforts have been adopted to enhance the separation performance of TiO₂, such as immobilization of TiO₂ onto various supports [11-18]. But the photocatalytic efficiency of pollutant degradation is usually decreased due to the mass transfer limitation when some materials without adsorption ability, such as glass and stainless steel are used as supports [13,14]. To enhance the mass transfer, some sorbents as the supporter of photocatalyst have drawn the attention of researchers. These sorbents used often contain silica gel [15], zeolite [11,17] and activated carbon (AC) [12,16,18]. Among them, AC is most commonly employed as catalyst support for TiO₂ due to its unique characteristics such as large specific surface area, highly developed porosity, strong adsorption capacity and superiority of low cost. Ao et al. [16] have prepared nanocrystal anatase TiO₂ particles deposited on AC at low temperature by sol-gel method. Their work showed that phenol pollutants were adsorbed by AC, and then migrated continuously onto the surface of TiO₂ for subsequent photocatalytic degradation. In the same vein, Ravichandran et al. [18] investigated the photocatalytic activity of immobilized commercial TiO₂ (Degussa P25) onto AC. Their results also indicated that there was a synergistic effect and a common interface, in which the adsorbed pollutants on AC were transferred to TiO₂-P25. Hence, when combining the roles of both adsorption and photocatalytic degradation, TiO₂/AC is expected to be a promising photocatalyst for the removal of organic pollutants from aqueous solution.

Furthermore, it was stated that the photocatalytic degradation efficiency of this process is dependent on numerous process parameters such as photocatalyst loading, initial substrate concentration, pH value, light intensity, air flow rate and presence of added oxidant species; working conditions are case-specific and need to be carefully optimized. The majority of recent studies concerned with the effects of these process parameters on the photocatalytic degradation

[†]To whom correspondence should be addressed.
E-mail: chrahman@eng.usm.my

efficiency were performed using a one-factor-at-a-time approach, where this approach assesses one parameter at a time instead of all simultaneously. The method is time consuming, expensive and often leads to misinterpretation of results when interactions between different components are present [19]. To overcome these drawbacks, one of the statistical design tools, so-called response surface methodology (RSM), can be used for process optimization and prediction of interaction between several process parameters and one or more dependent parameters. According to literature reports, RSM has been proven to be effective for the photocatalytic degradation process for wastewater treatment. Among them, one can refer, for instance, to the degradation of different dyes [20-22], metal ions [23,24] and other industrial effluents [19,25]. However, at the present time, there are limited studies dealing with the application of RSM that have been reported on the treatment of phenol present in wastewater.

Considering the above-mentioned facts, the present study aimed at investigating the photocatalytic degradation of phenol with TiO$_2$ deposited on granular activated carbon (TiO$_2$/GAC) prepared using a hydrothermal method. Its photocatalytic activity was evaluated in a fluidized bed reactor. RSM was applied to access the individual and interactive effects of several process parameters on the photocatalytic degradation efficiency. Central composite design (CCD), which was the most widely used form of RSM was employed to investigate the effects of important process parameters such as photocatalyst loading (layer), initial substrate concentration (mg L^{-1}) and H$_2$O$_2$ concentration (mg L^{-1}).

EXPERIMENTAL

1. Preparation of TiO$_2$/GAC

TiO$_2$ was prepared by a hydrothermal method [9] and subsequently immobilized on GAC. The procedure for the preparation of TiO$_2$/GAC was as follows: titanium tetraisopropoxide (TTIP, 98%+) was initially dissolved in isopropyl alcohol. After being stirred for 30 min, deionized water was added drop by drop under vigorous stirring. After being stirred for 30 min, HCl was then added to the mixture. The molar ratio of the mixture was 1 TTIP: 39.2 C$_3$H$_8$O: 1 H$_2$O: 0.08 HCl. The sol was further stirred for 2 h for the formation of a homogeneous solution. The resulting sol was then transferred into a stainless steel Teflon-lined autoclave for hydrothermal treatment (temperature: 180 °C, time: 2 h). The hydrothermally synthesized TiO$_2$ colloidal solution was used for the next coating process. Before 2 g of GAC (grain size about 1.2 mm) was used as the support, it was pre-washed with deionized water and dried in an oven at 60 °C for 12 h. The ratio of TiO$_2$ colloidal solution to GAC was 1 : 1 for the coating process. After coating, it was heated in an oven at 180 °C for 1 h. As a result, TiO$_2$/GAC was completed with a white layer on the surface of GAC. The process dip-coating to heat treatment was repeated to obtain the desired amount of deposited TiO$_2$. Finally, the amount of deposited TiO$_2$ was calculated by weighing the mass difference of GAC before and after deposition.

2. Catalyst Characterization

2-1. XRD, SEM and BET Analysis

XRD analysis of the TiO$_2$/GAC showed that the crystal phase of TiO$_2$ deposited on the surface of GAC was anatase, and the average crystallite size determined from the diffraction peak broadening by
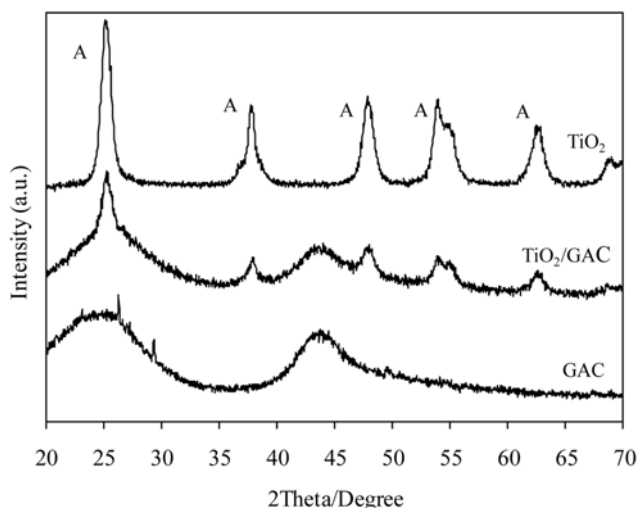

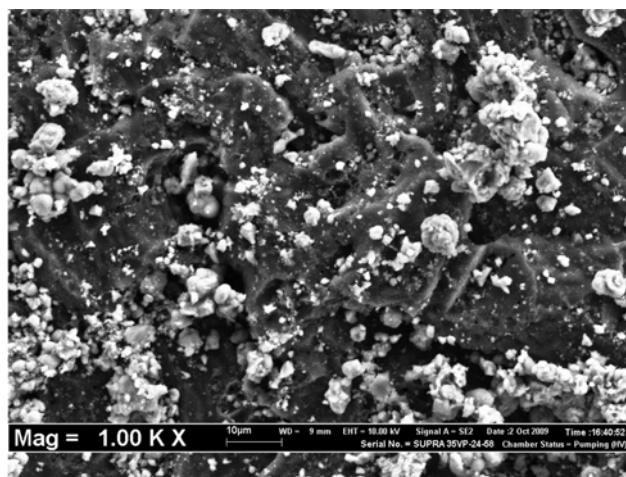Fig. 1. XRD patterns of GAC, TiO$_2$/GAC and TiO$_2$. (A: anatase).

Fig. 2. SEM image (×1,000) of TiO$_2$/GAC.

using the Scherer's formula [26] was 7.7 nm (Fig. 1). In addition, the SEM image (Fig. 2) of the catalyst indicated that agglomerated TiO$_2$ particles were well deposited on the surface of GAC and some of them were distributed within the GAC macro-pores. Furthermore, the BET surface area of TiO$_2$/GAC, TiO$_2$ and GAC was 840 m^2 g^{-1}, 50 m^2 g^{-1} and 873 m^2 g^{-1}, respectively, which indicated that the surface area of the TiO$_2$ had been enlarged after being deposited on GAC. On the other hand, the surface area of TiO$_2$/GAC was less when compared to GAC, because the deposited TiO$_2$ particles occupied the pores of GAC.

2-2. Photocatalytic Experiments

All photocatalytic experiments were carried out in a fluidized bed reactor (Fig. 3). A quartz glass column of about 55 mm in inner diameter, 60 mm in outer diameter and 600 mm in height was used as the main chamber for the photocatalytic reaction. The quartz column was surrounded by four 20 W germicidal UV lights (Sankyo Denki Co. Ltd.) with a maximum emission at 254 nm and total UV intensity measured by radiometer (Cole-Parmer, Series 9811) of 921 μW cm^{-2}. The UV lights and quartz column were enclosed in a stainless steel shield to avoid release of radiation and heat. 1,400
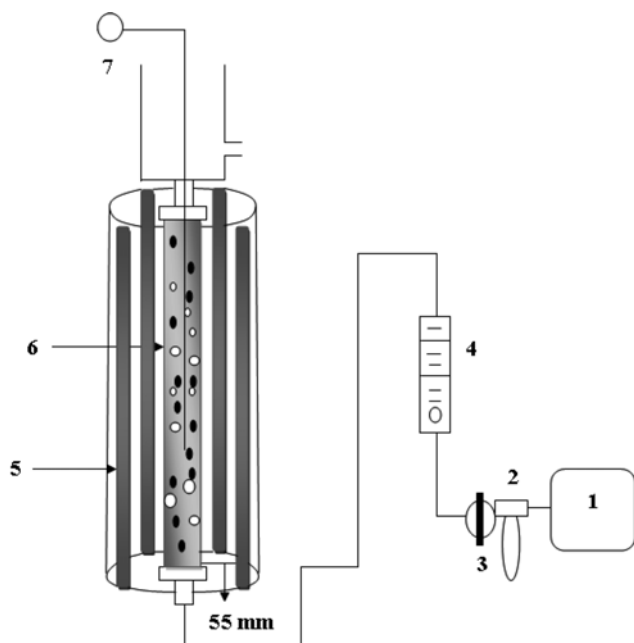
Fig. 3. Fluidized bed reactor. (1) air compressor; (2) air filter; (3) pressure gauge; (4) rotameter; (5) UV lamp; (6) quartz glass column and (7) thermocouple.

mL of phenol solution was implemented to the reactor each time, and H_2O_2 was also added to the reactor. An air diffuser was placed at the bottom of the reactor to uniformly disperse air into the solution and fluidized with air at a flow rate of $2\,L\,min^{-1}$. All experiments were conducted in batch mode and reaction temperature of $30\,°C$. Samples were withdrawn at the specific time intervals and filtered through $0.4\,\mu m$ millipore filters to remove the particles. The filtrate was then analyzed by HPLC (Perkin Elmer Series 200) using *C18* column (150 mm-length×4.6 mm-ID×5 μm-particle size) with a mobile phase mixture of water 60% (v/v) and acetonitrile 40% (v/v) at a flow rate of $1\,mL\,min^{-1}$. The wavelength of detector was set at 238 nm. To determine the reproducibility of the results, at least duplicated runs were carried out for each condition for averaging the results, and the experimental error was found to be within ±4%.

2-3. Experimental Design and Optimization

Experimental design of the photocatalytic degradation of phenol by TiO_2/GAC was carried out using the RSM. RSM is a collection of mathematical and statistical techniques that are useful for the modeling and analysis of problems in which a response of interest is influenced by several variables and the objective is to search optimum conditions for the response [27]. RSM consists of an empirical modeling technique devoted to the evaluation of relations existing between a group of controlled experimental factors and the observed results. RSM is a well-known efficient experimentation technique that has been applied in a wide range of chemical reactions and industrial processes for the purpose of either producing high quality products or operating the process in a more economical manner to ensure the process in a more stable and reliable way [28]. Whenever several input variables may influence the process performance measure, RSM can be utilized to assess the relationship between input variables (independent variables) and process performance measure (response) as well as to identify the optimum conditions for relevant processes.

In this study, a face-centered central composite design (CCD), which is a widely used form of RSM, was selected for the optimization of photocatalytic degradation of phenol using TiO_2/GAC. The CCD is an ideal design tool for sequential experimentation and allows testing the lack of fit when an adequate number of experimental values are available [27]. A three factorial and two level CCD (low (−1) and high (+1)), with six replicates at the center point leading to a total number of 20 experiments was employed for response surface modeling. The variables (independent factors) used in this experiment were the photocatalyst loading (x_1), initial phenol concentration (x_2) and H_2O_2 concentration (x_3). Phenol degradation efficiency (Y) was considered as the response (dependent factor). The real values of process variables and their variation limits were selected based on the values obtained in preliminary experiments and coded as shown in Table 1. Performance of the process was evaluated by analyzing the response of phenol degradation efficiency after 70 min of reaction.

In the optimization process, the responses can be simply related to chosen variables by linear or quadratic models. A quadratic model is given as follows:

$$Y = b_0 + \sum b_i x_i + \sum b_{ii} x_i^2 + \sum b_{ij} x_i x_j \qquad (1)$$

where Y is dependent response (phenol degradation efficiency, %); x_i and x_j are the independent variables; b_o, b_i (i=1, 2 and 3), b_{ii} and b_{ij} (i=1, 2 and 3; j=1, 2 and 3) are the model coefficients, respectively. Experimental results were analyzed using Design Expert software (DOE) version 6.0.6 (STAT-EASE Inc., Minneapolis, USA) and a regression model was proposed. Analysis of variance (ANOVA) was performed based on the proposed model to find the interaction between the process variables and the response. The quality of the fit for the polynomial model was expressed by the coefficient of determination (R^2, R^2_{adj}), and statistical significance was checked by the *F*-value (Fisher variation ratio), *P*-value and adequate precision in the same program. Model terms were selected or rejected based on the probability value with 95% confidence level. Finally, two-dimensional contour plots and three-dimensional response surface plots were drawn in order to visualize the individual and the interaction effects of the independent variables on phenol degradation.

Table 1. Experimental range and levels of independent variables

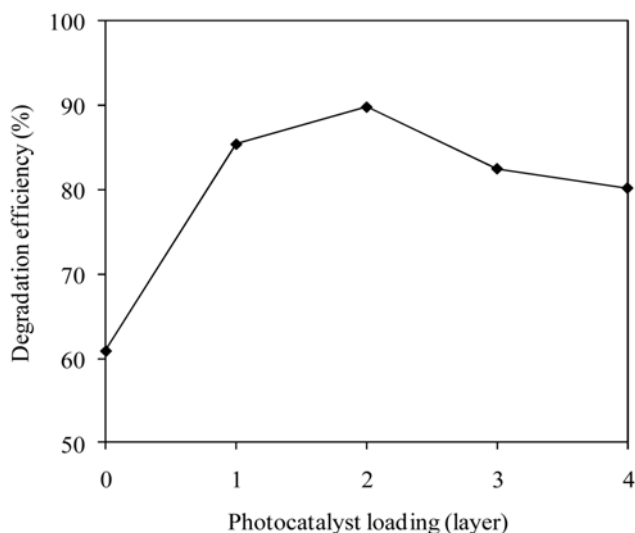| Variables	Coded	Range and levels		
		−1	0	+1
Photocatalyst loading (layer)	x_1	30	50	70
Initial phenol concentration (mg L^{-1})	x_2	1 (0.29 g L^{-1})	2 (0.32 g L^{-1})	3 (0.36 g L^{-1})
H_2O_2 concentration (mg L^{-1})	x_3	200	300	400

Fig. 4. Effect of photocatalyst loading on the photocatalytic degradation of phenol ([phenol]=50 mg L^{-1}; reaction time t=90 min).
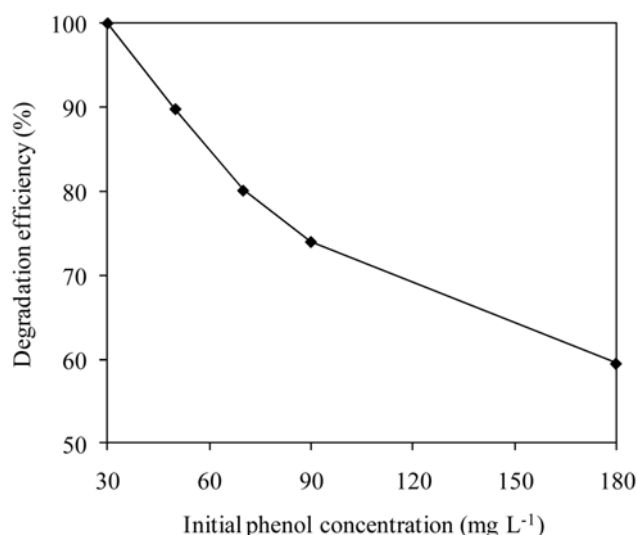

Fig. 5. Effect of initial phenol concentration on the photocatalytic degradation of phenol. (photocatalyst loading=two layers; reaction time t=90 min).

RESULTS AND DISCUSSION

1. Effect of Photocatalyst Loading

The influence of photocatalyst loading on the photocatalytic degradation of phenol was carried out by 1, 2, 3 and 4 photocatalyst coating layers corresponding to the photocatalyst loading of 0.29, 0.32, 0.36 and 0.39 g L^{-1} (weight of TiO₂ thin film per liter of solution), respectively. Fig. 4 shows the effect of photocatalyst loading on photocatalytic degradation of phenol. As can be seen in the figure, the degradation efficiency of phenol increased from 85.4% to 89.8% with photocatalyst loading from 0.29 to 0.32 g L^{-1}. However, at higher photocatalyst loadings as 0.36 and 0.39 g L^{-1}, the degradation efficiency of phenol decreased to 82.5% and 80.2%, respectively. This can be compared with 60.9% phenol loss for the same experiment carried out with GAC presence in the UV irradiation (absence of TiO₂). When investigating separate UV irradiation (photolysis) and GAC in the absence of UV light (adsorption), the phenol losses were 10.3% and 48.2%, respectively, in 90 min (diagram not shown). The phenol losses by photocatalysis degradation were much higher than those of photolysis and adsorption process, which implied that the combination of TiO₂ and GAC under UV irradiation can obtain a better performance. This phenomenon can be attributed to the TiO₂ loaded on GAC surface and will be further discussed in Section 3.6.
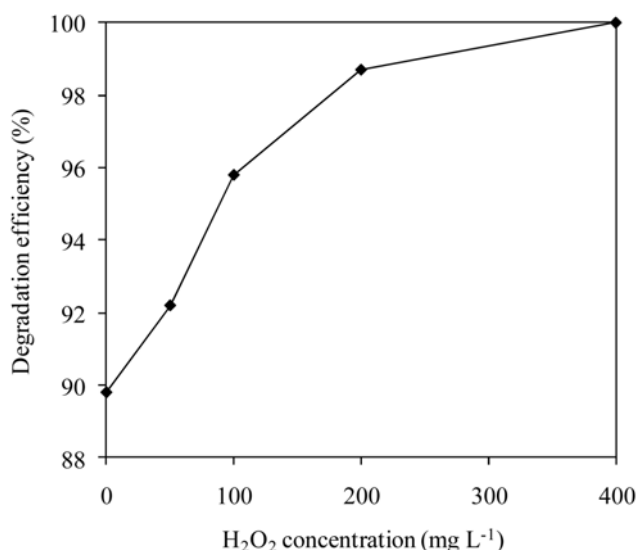
The effect of photocatalyst loading on the photocatalytic degradation of phenol can be explained in terms of the active sites on the TiO₂ available for photocatalytic degradation and the penetration of UV light into the deeper TiO₂ layers [11,17,29]. As the loading of photocatalyst increased, an increase in the number of active sites of TiO₂ was obtained. The increase in the number of photons absorbed and also the amount of phenol molecules adsorbed on the TiO₂ surface enhanced the photocatalytic degradation [29]. However, when the loading of photocatalyst was overdosed, the degradation efficiency of phenol decreased due to the interception of the UV light to reach the deeper TiO₂ layers. Mahalakshmi et al. [17] added that as the excess photocatalyst prevented the irradiation, •OH

radical as a primary oxidant in the photocatalytic system decreased and the efficiency of the degradation was reduced accordingly. Moreover, higher loading of TiO₂ also caused agglomeration of TiO₂ on the GAC support [17]; hence a part of the photocatalyst surface became unavailable for photon absorption and degradation efficiency of phenol decreased.

2. Effect of Initial Substrate Concentration

The dependency of photocatalytic degradation of phenol on the initial substrate concentration is presented in Fig. 5. The examined range of the initial phenol concentration varied from 30 to 180 mg L^{-1}. As can be seen, the initial phenol concentration had a pronounced effect on the amount of phenol degraded. At the same illumination time, the degradation efficiency of phenol decreased with increasing initial phenol concentration. For the initial phenol concentration of 30 mg L^{-1}, complete phenol degradation was observed after 90 min of reaction. Additionally, the phenol degradation efficiency was found to be 89.8%, 80.1%, 74.0% for the initial phenol concentrations of 50, 70 and 90 mg L^{-1}, respectively. In comparison, for the higher initial phenol concentration of 180 mg L^{-1}, 40.5% of phenol still remained in treated phenol after 90 min of reaction.

The initial substrate concentration dependence of the degradation efficiency of phenol could be attributed to three possible reasons: first, at high phenol concentrations, the generation of •OH radicals on the surface of catalyst is reduced [30]. The •OH radicals are formed by the reactions of valence band positive holes (h_{vb}^+) with adsorbed OH$^-$ anions and water. Since most of the active sites on the surface of TiO₂ are covered by phenol molecules at high phenol concentrations, there are only fewer active sites available for the adsorption of OH$^-$ anions. Second, with the increase in the phenol concentration, the UV light absorbed by the phenol is more than that of photocatalyst. Consequently, fewer photons managed to activate the photocatalyst surface for •OH radicals generation [31,32]. The third possible reason is the interference of intermediates formed upon the degradation of phenol. Sobczyński et al. [33] have reported that the intermediates such as hydroquinone, catechol, resorcinol and p-

Fig. 6. Effect of H₂O₂ on the photocatalytic degradation of phenol (photocatalyst loading=two layers; [phenol]=50 mg L⁻¹; reaction time t=90 min).

Fig. 6. Effect of H_2O_2 on the photocatalytic degradation of phenol (photocatalyst loading=two layers; [phenol]=50 mg L^{-1}; reaction time t=90 min).

benzoquinone formed during the phenol degradation were strongly adsorbed on the surface of photocatalyst and competed with phenol molecules for the same active sites on the surface of photocatalyst, thus inhibiting the degradation efficiency of phenol.

3. Effect of H₂O₂

The role of H_2O_2 in the photocatalytic degradation of phenol was studied in the range from 0 to 400 mg L^{-1}. Fig. 6 illustrates the effect of H_2O_2 on photocatalytic degradation of phenol. As can be seen, the degradation efficiency of phenol increased with increasing H_2O_2 concentration. After 90 min of reaction, the degradation efficiency of phenol increased from 89.8% to 98.7% with H_2O_2 concentration increased from 0 to 200 mg L^{-1}. At higher H_2O_2 concentration as 400 mg L^{-1}, complete degradation of phenol was observed after 90 min of reaction.

It has been well established that the major step of energy waste in the photocatalytic reaction of TiO_2 is the recombination of e_{cb}^--h_{vb}^+ pairs that leads to low quantum yield [32,34]. Hence, the prevention of e_{cb}^--h_{vb}^+ recombination becomes very important. This can be achieved by adding a proper electron acceptor such as H_2O_2 to the system. H_2O_2 can act as an alternative electron acceptor to oxygen to prevent the e_{cb}^--h_{vb}^+ recombination (Eq. (2)) [34]. Moreover, H_2O_2 also can react with the $O_2\bullet^-$ radicals, increasing the generation of $\bullet OH$ radicals (Eq. (3)) [35].

$$H_2O_2 + e_{cb}^- \rightarrow \bullet OH + OH^- \tag{2}$$

$$H_2O_2 + O_2\bullet^- \rightarrow \bullet OH + OH^- + O_2 \tag{3}$$

Further, H_2O_2 also can split photocatlytically to generate $\bullet OH$ radicals via UV irradiation at 254 nm (Eq. (4)). Irmak et al. [36] reported that the increasing in efficiency of photocatalytic degradation after the addition of H_2O_2 was ascribed to the extra formation of $\bullet OH$ radicals due to hemolytic cleavage of bonds holding two hydroxyl groups during the photolysis.

$$H_2O_2 + h\nu \rightarrow 2\bullet OH \tag{4}$$

Table 2. Experimental and predicted degradation efficiency of phenol (%)

Run	Variables			Response (%)	
	x_1	x_2	x_3	Y	Y_{pred}
1	−1	−1	−1	95.8	95.8
2	1	−1	−1	94.1	93.8
3	−1	1	−1	90.6	90.4
4	1	1	−1	84.2	84.6
5	−1	−1	1	100	99.5
6	1	−1	1	100	100
7	−1	1	1	95.1	95.3
8	1	1	1	92.2	92.0
9	−1	0	0	92.7	93.3
10	1	0	0	90.6	90.7
11	0	−1	0	99.1	99.9
12	0	1	0	93.3	93.2
13	0	0	−1	93.7	93.8
14	0	0	1	98.9	99.4
15	0	0	0	96.8	95.6
16	0	0	0	95.8	95.6
17	0	0	0	94.5	95.6
18	0	0	0	95.6	95.6
19	0	0	0	96.9	95.6
20	0	0	0	95.3	95.6

As expected, H_2O_2 showed a beneficial effect on the photocatalytic degradation of the phenol under investigation as evident from Fig. 6.

4. Central Composite Design Experiment

Table 2 shows the CCD with photocatalyst loading, initial phenol concentration and H_2O_2 for 20 experimental runs. The observed degradation efficiency of phenol varied between 84.2% to 100%, and the model predictions matched these experimental results satisfactorily. The result obtained after CCD was then analyzed by standard analysis of variance (ANOVA), which gave the following regression equation (in terms of coded factors) (Eq. (5)):

$$Y = 95.60 - 1.31\,x_1 - 3.36\,x_2 + 2.78\,x_3 - 3.63\,x_1^2 + 0.92\,x_2^2 + 1.02\,x_3^2 - 0.95\,x_1x_2 + 0.65\,x_1x_3 + 0.65\,x_2x_3 \tag{5}$$

where x_1, x_2 and x_3 represent photocatalyst loading, initial phenol concentration and H_2O_2 concentration, respectively.

ANOVA results of this model for phenol degradation are summarized in Table 3. The degree of significance of each variable is represented in this table by its P-value. When a variable has a P-value smaller than 0.05, it influences the degradation efficiency of phenol response at a confidence level of 0.95. It can be seen from Table 3 that the linear effects of photocatalyst loading (x_1), initial phenol concentration (x_2) and H_2O_2 concentration (x_3), second order effect of photocatalyst loading (x_1^2), as well as interaction effects of photocatalyst loading with initial phenol concentration (x_1x_2) and photocatalyst loading with H_2O_2 concentration (x_1x_3) were significant factors. Other than that were said to be insignificant as the P-value is greater than 0.0500. However, these model terms are not eliminated from the analysis. Montgomery [27] reported that eliminating these terms would reduce the dimensionality of the response surface and consequently the misinterpretation would occur more

Table 3. Analysis of variance (ANOVA) for the degradation efficiency of phenol (%)

| Source	Sum of squares	Freedom degree	Mean square	F-Value	P-Value
Model	257.26	9	28.58	45.14	<0.0001
x_1	17.16	1	17.16	27.10	0.0004
x_2	112.90	1	112.90	178.28	<0.0001
x_3	77.28	1	77.28	122.04	<0.0001
x_1^2	36.18	1	36.18	57.14	<0.0001
x_2^2	2.34	1	2.34	3.70	0.0834
x_3^2	2.88	1	2.88	4.54	0.0589
x_1x_2	7.22	1	7.22	11.40	0.0070
x_1x_3	3.38	1	3.38	5.34	0.0435
x_2x_3	0.72	1	0.72	1.14	0.3114
Residual	6.33	10	0.63		
Lack of fit	2.14	5	0.43	0.51	0.7600
Pure error	4.19	5	0.84		

$R^2=0.9760$, $R_{adj}^2=0.9544$, Std. Dev.=0.80, Mean=94.76, Adeq. Precision=27.511, C.V.=0.84

easily. The accuracy and variability of the model can be evaluated by the coefficient of determination R^2. The R^2 value is always between 0 and 1. The closer the R^2 value to 1, the stronger the model is and the better the model predicts the response [37]. As can be seen from Table 3, the R^2 value 0.9760 for phenol degradation, which implied that 97.60% of variations were explained by the independent vari-
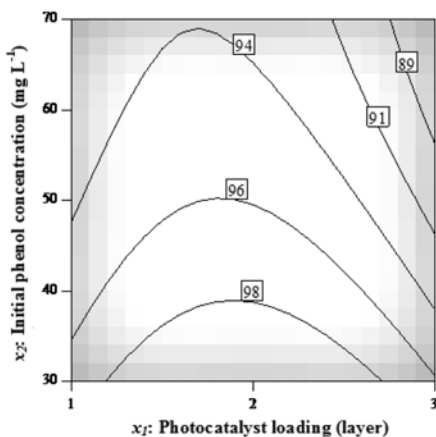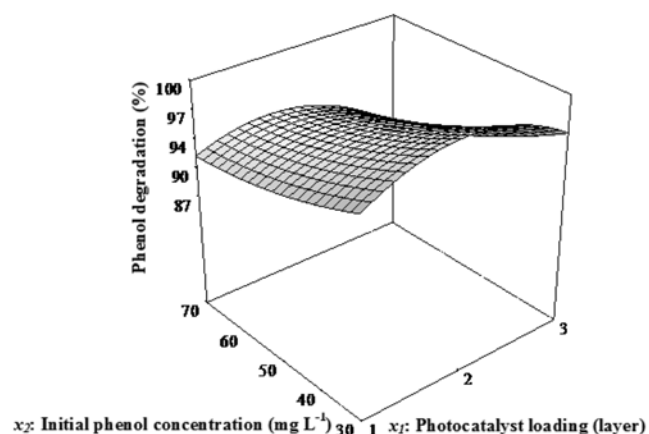
Fig. 7. Response surface and contour plots of degradation efficiency of phenol (Y%) for t=70 min as a function of photocatalyst loading (x_1) and initial phenol concentration (x_2) in fixed H₂O₂ concentration (x_3) at 300 mg L⁻¹.
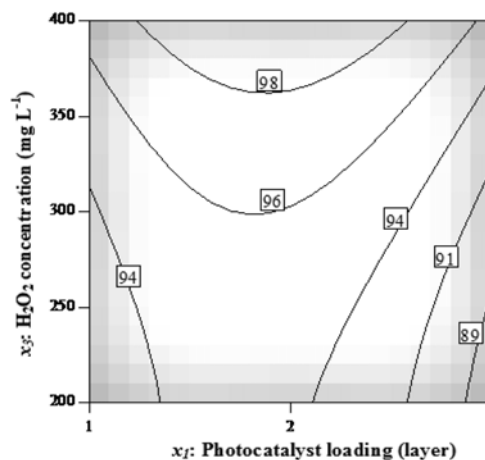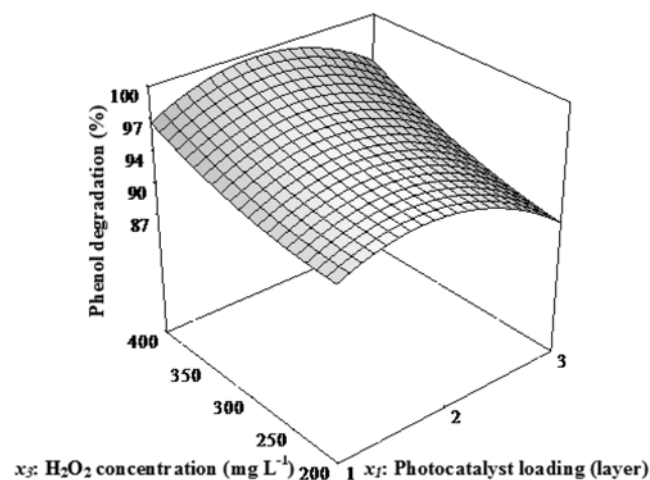
Fig. 8. Response surface and contour plots of degradation efficiency of phenol (Y%) for t=70 min as a function of photocatalyst loading (x_1) and H₂O₂ concentration (x_3) in fixed initial phenol concentration (x_3) at 50 mg L⁻¹.

ables within the range studied and only 2.40% of the total variations cannot be explained by the model. Moreover, the adjusted determination coefficient R^2_{adj} value 0.9544 was also very high, which suggested excellent correlations between the independent variables. Adequate precision is a measure of the range in predicted response relative to its associated error or, in other words, a signal to noise ratio. A value greater than 4 is desirable in supporting the fitness of the model [28]. According to the data in Table 3, the value of adequate precision of 27.511 was found desirable. Simultaneously, low value of the coefficient of variation (C.V.=0.84), indicated good precision and reliability of the experiments.

After performing statistical analyses, the response surface analysis was carried out in order to find the optimum conditions for the degradation efficiency of phenol. Figs. 7-9 show the response surface plots and contours for the optimization conditions of phenol degradation. In each plot, two variables are varied while the third variable is kept constant. From the response surface plots and con-

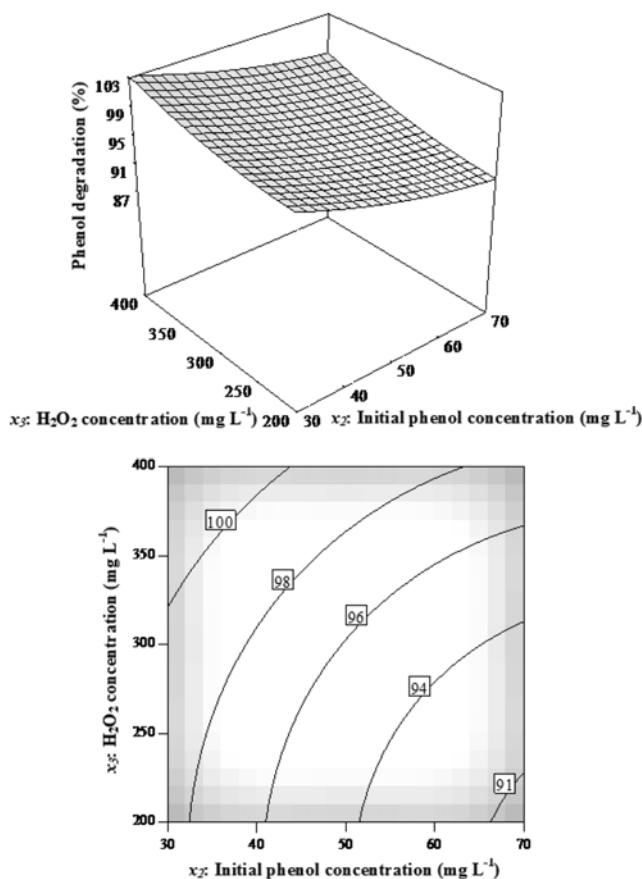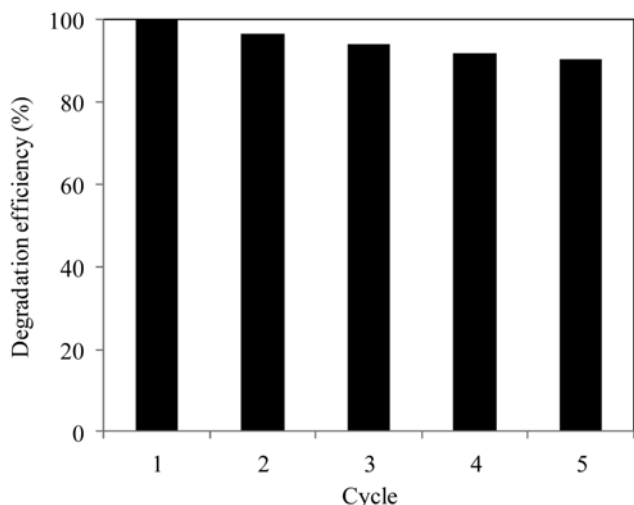**Fig. 9. Response surface and contour plots of degradation efficiency of phenol (Y%) for t=70 min as a function of initial phenol concentration (x_2) and H_2O_2 concentration (x_3) in fixed photocatalyst loading (x_1) at two layers.**

tours, it is easy and convenient to understand the interaction between the three variables and optimum condition of each variable required for maximum phenol degradation. The effect of photocatalyst loading and initial phenol concentration at 300 mg L^{-1} H_2O_2 are illustrated in Fig. 7. As can be seen, degradation efficiency of phenol increased with the decrease in initial phenol concentration at 300 mg L^{-1} H_2O_2. Fig. 8 shows the effect of photocatalyst loading and H_2O_2 concentration on phenol degradation, and shows that phenol degradation increased with the increase in H_2O_2 concentration at zero level of initial phenol concentration. In Figs. 7 and 8, the degradation efficiency of phenol is very sensitive to the change of photocatalyst loading. The degradation efficiency of phenol increases up to a certain limit (2 layers) and then decreases with increasing photocatalyst loading. Fig. 9 shows the effect of initial phenol concentration and H_2O_2 concentration at photocatalyst loading of two layers. It can be seen that the degradation efficiency of phenol increased with increasing H_2O_2 concentration and decreasing initial phenol concentration. Complete phenol degradation was obtained at 30 mg L^{-1} initial phenol concentration and 400 mg L^{-1} H_2O_2 at two layers of photocatalyst loading.

To validate the model, an experiment was carried out under predicted conditions, and the observed value for the degradation efficiency of phenol is presented in Table 4. The experimental degradation efficiency of phenol was 99.9%, which highly agreed with that 99.5% predicted by the equation. The optimum conditions of phenol degradation were obtained with photocatalyst loading of two layers, initial phenol concentration of 34.44 mg L^{-1} and H_2O_2 concentration of 326.90 mg L^{-1}. As compared with the results obtained from one-factor-at-a-time experiments, the optimum conditions were photocatalyst loading of two layers, initial phenol concentration of 30 mg L^{-1} and H_2O_2 concentration of 400 mg L^{-1}. This implied that the quadratic regression model reasonably optimized the variable conditions and predicted the degradation efficiency of phenol.

5. Recycling Catalytic Ability of TiO₂/GAC

Recycling use of photocatalyst is very important for the practical applications. To evaluate the stability of TiO₂/GAC, recycling experiments were carried out under the optimal conditions based on the results from the CCD model. For each new cycle, the photocatalyst was filtered, washed and left at room temperature during 24 h. The results are shown in Fig. 10. At the first cycle, 99.9% phenol was degraded. As increasing recycling times, the efficiency of phenol degradation decreased slightly, which was still higher than 90% after being used for five cycles. The results revealed that the photocatalytic activity of TiO₂/GAC has repeatability. Similar results were also obtained in other studies on TiO₂ immobilized AC system [16, 38]. Ao et al. [16] reported that the reduction in efficiency of photocatalytic degradation after being reused was ascribed to the formation of intermediates and their accumulation on the surface of the photocatalyst. On the other hand, the TiO₂ deposited on GAC almost did not release or dissolve into the solution, indicating that

Table 4. Validation of the model

| Photocatalyst loading x_1 (layer)	Initial phenol concentration x_2 (mg L^{-1})	H_2O_2 concentration x_3 (mg L^{-1})	Degradation efficiency (%)	
			Predicted	Experimental
2	34.44	326.90	99.5	99.9

Fig. 10. Photocatalytic efficiency of TiO₂/GAC for phenol degradation of five cycles (photocatalyst loading=two layers; [phenol]=34.44 mg L⁻¹; [H₂O₂]=326.90 mg L⁻¹; reaction time t=70 min).

the deposited TiO_2 was very stable.

6. Migration of Phenol from GAC to TiO₂ under UV Irradiation

Taking into account the fact that both the adsorption and degradation of phenol occurred in the as prepared TiO_2/GAC, efforts have been made to determine the quantity of phenol remaining on the solid. In the present study, a method reported by Ao et al. [16] was followed. After each certain reaction time, the solids in the absence and presence of UV light were subjected to solvent extraction with 1 L of acetonitrile under sonication for 20 min. The results are shown in Fig. 11. Blank preliminary experiments performed on GAC in the absence of UV light have shown that phenol could be extracted from GAC with extracted concentration for 90 min being 20.6 mg
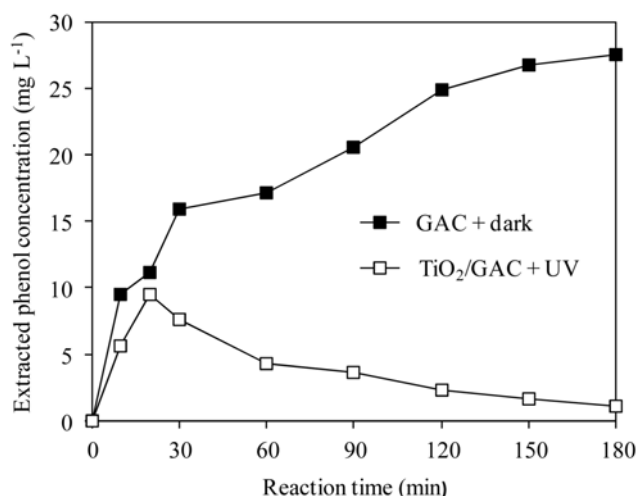
Fig. 11. Concentration of phenol extracted from GAC and TiO₂/GAC after being exposed to phenol solution for different reaction times in the absence and presence of UV light, respectively (photocatalytic loading=2 layers; [phenol]=50 mg L⁻¹).

L^{-1}. This concentration was much higher than the extracted one (3.2 mg L^{-1}) from the illuminated TiO_2/GAC. In addition, the extracted concentration from GAC in the absence of UV light increased gradually with increasing reaction time, while the extracted concentration from the illuminated TiO_2/GAC reached maximum and then decreased rapidly. After the reaction time was prolonged to 180 min, the quantity of phenol remaining adsorbed on the illuminated TiO_2/GAC was reduced to nearly zero.

Since GAC has no photoactivity, the TiO_2 particles deposited on the GAC must have played an important role in enhancing the continuous degradation of phenol in the presence of UV light. The decrease in the extracted concentration can be explained by the phenol molecules that have been adsorbed and accumulated on the GAC during the photocatalytic degradation were able to migrate to the surface of TiO_2, where they were degraded under UV irradiation. Similar results were also reported by other researchers in the photocatalytic degradation of phenol and other pollutant using TiO_2/AC [16,39].

CONCLUSIONS

The photocatalytic degradation of phenol in the presence of TiO_2/GAC was investigated in this study, focusing on the influence of some parameters such as photocatalyst loading, initial substrate concentration and addition of an oxidizing agent as H_2O_2. The experimental results demonstrated that an optimum photocatalyst loading of two layers was needed to achieve a high degradation efficiency of phenol. The photocatalysis worked best at low substrate concentration as the degradation efficiency decreased with increasing initial phenol concentration. Addition of H_2O_2 can have a positive effect on the degradation efficiency of phenol.

Using response surface methodology (RSM) to create a set of experimental runs can reduce the number of runs required to optimize the process variables compared with the one-factor-at-a-time experiment method. This method provided sufficient statistical data to fit the quadratic model for photocatalytic degradation of phenol. Accordingly, the optimum conditions provided by the model were at photocatalyst loading of two layers, initial phenol concentration of 34.44 mg/L and H_2O_2 concentration of 326.90 mg/L. In comparison, for those obtained by the one-factor-at-a-time experiments, RSM based on central composite design could be effectively adopted to optimize the process multivariable and maximize the degradation efficiency of phenol. The TiO_2/GAC was used for five cycles with phenol degradation efficiency still higher than 90%. Finally, phenol adsorbed to the surface of the GAC was able to migrate continuously onto the surface of TiO_2, which enhanced the phenol degradation efficiency greatly.

ACKNOWLEDGEMENTS

REFERENCES

1. M. Tasbihi, C. R. Ngah, N. Aziz, A. Mansor, A. Z. Abdullah, K. T.

J.-C. Sin et al.

Lee and A. R. Mohamed, *Ind. Eng. Chem. Res.*, **46**, 9006 (2007).

2. M. Bertelli and E. Selli, *J. Hazard. Mater.*, **B138**, 46 (2006).

3. A. Kumar, S. Kumar, S. Kumar and D. V. Gupta, *J. Hazard. Mater.*, **147**, 155 (2007).

4. B. H. Hameed and A. A. Rahman, *J. Hazard. Mater.*, **160**, 576 (2008).

5. M. L. Chin, A. R. Mohamed and S. Bhatia, *Chemosphere*, **57**, 547 (2004).

6. P. Saravanan, K. Pakshirajan and P. Saha, *J. Hydro-environ.*, **3**, 45 (2009).

7. G. Marcì, A. Sclafani, V. Augugliaro, L. Palmisano and M. Schiavello, *J. Photochem. Photobio. A: Chem.*, **89**, 69 (1995).

8. W. F. Jardim, S. G. Moraes and M. M. K. Takiyama, *Water Res.*, **31**, 1728 (1997).

9. M. Kang, *Appl. Catal. B: Environ.*, **37**, 187 (2002).

10. B. X. Zhao, X. Z. Li and P. Wang, *J. Environ. Sci.*, **19**, 1020 (2007).

11. A. N. Okte and O. Yilmaz, *Appl. Catal. B: Environ.*, **85**, 92 (2008).

12. Z. He, S. G. Yang, Y. M. Ju and C. Sun, *J. Environ. Sci.*, **21**, 268 (2009).

13. A. Fernández, G. Lassaletta, V. M. Jiménez, A. Justo, A. R. González-Elipe, J. M. Herrmann, H. Tahiri and Y. Ait-Ichou, *Appl. Catal. B: Environ.*, **7**, 49 (1995).

14. J. Shang, W. Li and Y. F. Zhu, *J. Mol. Catal. A: Chem.*, **202**, 187 (2003).

15. Y. M. Wang, S. W. Liu, Z. L. Xiu, X. B. Jiao, X. P. Cui and J. Pan, *Mat. Lett.*, **60**, 974 (2006).

16. Y. H. Ao, J. J. Xu, D. G. Fu, X. W. Shen and C. W. Yuan, *Colloids Surf. A: Physicochem. Eng. Aspects*, **312**, 125 (2008).

17. M. Mahalakshmi, S. V. Priya, B. Arabindoo, M. Palanichamy and V. Murugesan, *J. Hazard. Mater.*, **161**, 336 (2009).

18. L. Ravichandran, K. Selvam and M. Swaminathan, *J. Mol. Catal. A: Chem.*, **317**, 89 (2010).

19. Y. X. Lin, C. Ferronato, N. S. Deng, F. Wu and J. M. Chovelon, *Appl. Catal. B: Environ.*, **88**, 32 (2009).

20. H. L. Liu and Y. R. Chiou, *Chem. Eng. J.*, **112**, 173 (2005).

21. I. H. Cho and K. D. Zoh, *Dyes Pigments*, **75**, 533 (2007).

22. C. Betianu, F. A. Caliman, M. Gavrilescu, I. Cretescu, C. Cojocaru and I. Poulios, *J. Chem. Technol. Biotech.*, **83**, 1454 (2008).

23. Y. G. Tao, L. B. Ye, J. Pan, Y. M. Wang and B. Tang, *J. Hazard. Mater.*, **161**, 718 (2009).

24. M. C. Yeber, C. Soto, R. Riveros, J. Navarrete and G. Vidal, *Chem. Eng. J.*, **152**, 14 (2009).

25. V. A. Sakkas, P. Calza, M. A. Islam, C. Medana, C. Baiocchi, K. Panagiotou and T. Albanis, *Appl. Catal. B: Environ.*, **90**, 526 (2009).

26. X. J. Wang, Z. H. Hu, Y. J. Chen, G. H. Zhao, Y. F. Liu and Z. B. Wen, *Appl. Surf. Sci.*, **255**, 3953 (2009).

27. D. C. Montgomery, *Design and analysis of experiments*, John Wiley & Sons, New York (1991).

28. I. Arslan-Alaton, G. Tureli and T. Olmez-Hanci, *J. Photochem. Photobio. A: Chem.*, **202**, 142 (2009).

29. W. Liu, S. F. Chen, W. Zhao and S. J. Zhang, *Desalination*, **249**, 1288 (2009).

30. C. G. Silva and J. L. Faria, *J. Mol. Catal. A: Chem.*, **305**, 147 (2009).

31. C. H. Wu, *Dyes Pigments*, **77**, 31 (2008).

32. N. Kashif and F. Ouyang, *J. Environ. Sci.*, **21**, 527 (2009).

33. A. Sobczyński, Ł. Duczmal and W. Zmudziński, *J. Mol. Catal. A: Chem.*, **213**, 225 (2004).

34. H. K. Singh, M. Saquib, M. M. Haque and M. Muneer, *J. Hazard. Mater.*, **142**, 374 (2007).

35. R. R. Ishiki, H. M. Ishiki and K. Takashima, *Chemosphere*, **58**, 1461 (2005).

36. S. Irmak, E. Kusvuran and O. Erbatur, *Appl. Catal. B: Environ.*, **54**, 85 (2004).

37. R. Kaushik, S. Saran, J. Isar and R. K. Saxena, *J. Mol. Catal. B: Enzymatic*, **40**, 121 (2006).

38. S. X. Liu, X. Y. Chen and X. Chen, *J. Hazard. Mater.*, **143**, 257 (2007).

39. D. K. Lee, S. C. Kim, I. C. Cho, S. J. Kim and S. W. Kim, *Sep. Purif. Technol.*, **34**, 59 (2004).